Korean J. Chem. Eng., **27**(6), 1868-1875 (2010)
DOI: 10.1007/s11814-010-0309-1

Chemical absorption of carbon dioxide into phenyl glycidyl ether solution containing THA-CP-MS41 catalyst

Young-Son Choe*, Kwang-Joong Oh, Min-Chul Kim**, and Sang-Wook Park*,†**

*Division of Chemical and Biomolecular Engineering, Pusan National University, Busan 609-735, Korea
**Division of Civil and Environmental Engineering, Pusan National University, Busan 609-735, Korea
(*Received 26 November 2009 • accepted 12 April 2010*)

Abstract−Carbon dioxide was absorbed into the phenyl glycidyl ether (PGE) solution within a range of 0-2.0 kmol/m^3 in a stirred batch tank with a planar gas-liquid interface at 333-363 K and 101.3 kPa. Trihexylamine-immobilized on chloropropyl-functionalized MCM-41 (THA-CP-MS41) was used as a mesoporous catalyst, dispersed in organic liquid for the reaction between carbon dioxide and PGE. The measured absorption rates were analyzed to obtain the reaction kinetics of the consecutive chemical reactions which consisted of two steps using the mass transfer mechanism based on film theory. The overall reaction kinetics, analyzed with the pseudo-first-order reaction constant in the consecutive reaction model, was equivalent to the consecutive reaction kinetics. Effects of polar solvent, such as *N*, *N*-dimethylacetamide, *N*-methyl-2-pyrrolidinone, and dimethyl sulfoxide, on the reaction rate constants were observed using the solubility parameter of the solvent.

Key words: Absorption, Carbon Dioxide, Phenyl Glycidyl Ether, Trihexylamine, MCM-41

INTRODUCTION

The chemical fixation of carbon dioxide has received much attention in view of environmental problems. An attractive strategy to deal with this situation is converting carbon dioxide into valuable substances. The reaction of CO_2 with oxiranes leading to 5-membered cyclic carbonates is well known [1], whereby these subsequent carbonates can be used as polar aprotic solvents, electrolytes for batteries, and sources of reactive polymers [2].

The synthesis of cyclic carbonates by the reaction of CO_2 with oxirane has been performed using Lewis acids, transition metal complexes, and organometallic compounds as catalysts at high pressures, 10-50 atmospheres [3,4]. Milder conditions, however, atmospheric pressure in the presence of metal halides or quaternary onium salts, have been reported [5-10].

The papers [3-9] regarding oxirane-CO_2 reactions have focused on the reaction mechanism, the overall reaction kinetics, and the effect of the catalyst on the conversion. Because the diffusion may have an effect on the reaction kinetics [11] in the mass transfer accompanied by chemical reactions, we believe it worthwhile to investigate this effect on the reaction kinetics of the gas-liquid heterogeneous reaction between CO_2 and oxirane.

A variety of functionalized catalysts such as polymers, amorphous, and fumed silica shows mild activity due to low accessibility for low/non porosity. The discovery of the M41S family by a Mobil scientist [12,13] generated a great deal of interest in the synthesis of organically-functionalized, mesoporous materials for their application in the fields of catalysis, sensing, and adsorption, given their high surface areas and large ordered pores ranging from 20 to 100 Å [12-14] with narrow size distributions. High chemical and thermal stabilities also make them potentially promising candidates for the reactions of bulky substrate molecules. In general, hybrid organic-inorganic materials have been prepared *via* post-grafting or co-condensation techniques. In 2000, Bhaumik and Tatsumi [15] reported a grafting technique through a co-condensation method for hybrid MCM-41 using halogenated organosilanes. Recently, a new synthetic approach has been developed for the preparation of hybrid inorganic-organic mesoporous materials based on the co-condensation of siloxane and organosiloxane precursors in the presence of different templating surfactant solutions [16-19]. Udayakumar et al. [20] reported a new grafting technique for the synthesis of hybrid MCM-41 and trialkylamine-immobilized ionic liquids containing high catalytic activity for the synthesis of cyclic carbonates.

Park et al. have studied the kinetics of the reaction between CO_2 and oxiranes, such as phenyl glycidyl ether (PGE) and glycidyl methacrylate, using catalysts such as Alquat 336 [21,22], 18-crown-6 [23], tetrabutylammonium bromide [24], tetrabutylammonium chloride [25], tetraethylammonium chloride [26], and triethylamine-immobilized ionic liquid on hybrid MCM-41 [27] in series. They presented a method how to obtain the reaction rate constants using the measured absorption rate of CO_2, analyzed with the mass transfer mechanism accompanied by chemical reactions, which consisted of two steps: a reversible reaction between oxirane and the catalyst to form an intermediate complex, and an irreversible reaction between the intermediate complex and CO_2 to form the catalyst and five-membered cyclic carbonate. But they did not consider the overall reaction kinetics between CO_2 and oxirane.

To our knowledge, no literature report about absorption kinetics using a catalyst of trialkylamine-immobilized ionic liquid on hybrid MCM-41 to utilize CO_2 has yet been published except the article [27] of Park et al., as mentioned above. In this study, PGE and the mesoporous particle trihexylamine-immobilized ionic liquid on the hybrid MCM-41 (THA-CP-MS41) [20] were used as a reactant and

†To whom correspondence should be addressed.
E-mail: swpark@pusan.ac.kr

a catalyst, respectively, which is one of the series of works to investigate the absorption kinetics of CO_2 in a heterogeneous system. Also, the reaction kinetics of the consecutive reaction with 2-step was compared with those of the overall reaction.

THEORY

1. Consecutive Reaction Model

To determine the reaction kinetics between PGE and carbon dioxide using a quaternary onium salt catalyst such as THA-CP-MS41, it is necessary to understand the absorption mechanism in a heterogeneous system. Although the reaction mechanism shown in Eq. (i) has been proposed by many researchers for homogeneous [3,6-9] and heterogeneous [20] oxirane-CO_2 reactions, no reliable evidence has yet been reported. It has been found that the rate-determining step is the attack of the anionic portion of the catalyst on the oxirane. The importance of this portion of the catalyst can be explained by this mechanism, whereby the overall reaction between CO_2 and PGE to form the 5-membered cyclic carbonate is as follows:

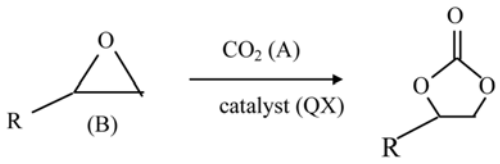

(i)

where R is a functional group of $-CH_2-O-C_6H_5$. The overall reaction of Eq. (i) in this study is assumed to consist of two consecutive steps: i) a reversible reaction between PGE (B) and THA-CP-MS41 (QX) to form an intermediate complex (C_1), ii) An irreversible reaction between C_1 and CO_2 (A) to form QX and five-membered cyclic carbonate (C):

$$B + QX \underset{k_2}{\overset{k_1}{\leftrightarrow}} C_1 \tag{ii}$$

$$A + C_1 \xrightarrow{k_3} C + QX \tag{iii}$$

The consecutive chemical reaction rate of CO_2 under the condition of a steady-state approximation to form C_1 is presented as follows:

$$r_{A,cons} = \frac{C_B S_t}{\frac{1}{k_1} + \frac{1}{K_1 k_3 C_A} + \frac{C_B}{k_3 C_A}} \tag{1}$$

If the value of k_1 is very large, such that $1/k_1$ approaches 0, Eq. (1) is arranged to

$$r_{A,cons} = \frac{K_1 k_3 C_A C_B S_t}{1 + K_1 C_B} \tag{2}$$

Under the assumptions that B is a nonvolatile solute, the gas phase resistance to absorption is negligible by using pure CO_2, and Raoult's law is thus applied. The mass balances of CO_2 and PGE, using film theory accompanied by the consecutive chemical reactions, and boundary conditions are given as follows:

$$D_A \frac{d^2 C_A}{dz^2} = r_{A,cons} \tag{3}$$

$$D_B \frac{d^2 C_B}{dz^2} = r_{A,cons} \tag{4}$$

$$z = 0;\ C_A = C_{Ai};\ \frac{dC_B}{dz} = 0 \tag{5}$$

$$z = z_L;\ C_A = C_{AL};\ C_B = C_{B0} \tag{6}$$

If the diffusion rate of CO_2 is not smaller than the reaction rate, and the amount of dissolved CO_2 that reacts in the diffusion film adjacent to the phase boundary is negligible, compared to that which reaches the bulk liquid phase in the unreacted state, the CO_2 concentration in the bulk liquid phase is a finite quantity (C_{AL}) that can be obtained from the following Eq. (11):

$$k_{Loc} a_V (C_{Ai} - C_{AL}) = \frac{K_1 k_3 C_{AL} C_{Bo} S_t}{1 + K_1 C_{Bo}} \tag{7}$$

The enhancement factor of CO_2, defined as the ratio of the flux of CO_2 with chemical reaction to that without chemical reaction, is shown as follows:

$$\beta = -\left.\frac{da}{dx}\right|_{x=0} \tag{8}$$

where $a = C_A/C_{Ai}$ and $x = z/z_L$

At the initial absorption of CO_2, C_B in the liquid film is constant as C_{Bo} and Eq. (2) for the reaction between CO_2 and PGE is arranged as

$$r_{A1} = k_o C_A \tag{9}$$

and the pseudo-first-order reaction rate constant becomes Eq. (10) and Eq. (11)

$$k_o = \frac{K_1 k_3 S_t C_{Bo}}{1 + K_1 C_{Bo}} \tag{10}$$

$$\frac{C_{Bo} S_t}{k_o} = \frac{1}{K_1 k_3} + \frac{C_{Bo}}{k_3} \tag{11}$$

The mass balance of CO_2 with the film theory accompanied by a pseudo-first-order reaction is given as follows:

$$D_A \frac{d^2 C_A}{dz^2} = k_o C_A \tag{12}$$

From the exact solution of Eq. (11), β is presented as follows:

$$\beta = \frac{Ha}{\tanh Ha} \tag{13}$$

where Ha is the Hatta number, $\sqrt{k_o D_A}/k_{Loc}$.

2. Overall Reaction Model

The overall reaction between CO_2 and PGE in reaction (i) to form the 5-membered cyclic carbonate is as follows:

$$A + B \xrightarrow{k_{overall}} C \tag{14}$$

The overall reaction rate of CO_2 is

$$r_{A,over} = k_{over} C_A C_B \tag{15}$$

Under the condition of the pseudo-first-order reaction, $r_{A,over}$ of (15) is equal to r_{A1} of Eq. (9), and then, k_{over} is given as follows:

$$k_{over} = \frac{k_o}{C_{Bo}} = \frac{k_{max} S_t}{1 + K_1 C_{Bo}} \tag{16}$$

where k_{max} is $K_1 k_3$, defined as the specific overall reaction rate con-

stant with maximum of k_{over}. As shown in Eq. (16), k_{over}, is a form similar to Michaelis-Menten enzyme kinetics or the Langmuir adsorption isotherm.

The mass balances of CO_2 and PGE based on film theory accompanied by the overall chemical reaction are used as follows:

$$D_A \frac{d^2C_A}{dz^2} = r_{A,over} \quad (17)$$

$$D_B \frac{d^2C_B}{dz^2} = r_{A,over} \quad (18)$$

β_{over} can be estimated using Eq. (8) and the solution of the differential equations of Eq. (17) and (18) with the boundary conditions of Eq. (5) and (6).

EXPERIMENTAL

1. Chemicals

All chemicals were of reagent grade and were used without further purification. Purity of both CO_2 and N_2 was greater than 99.9%. PGE, trihexylamine, bromoethane, tetraorthosilicate, 3-chloropropyltriethoxysilane, cetyltrimethylammonium bromide, tetramethylammounium chloride, and solvents such as *N*, *N*-dimethylacetamide (DMA), *N*-methyl-2-pyrrolidinone (NMP), and dimethyl sulfoxide (DMSO) were supplied by Aldrich chemical company, U.S.A.

2. Absorption Rate of CO_2

Absorption experiments were carried out in an agitated vessel and the experimental procedure duplicated in detail as previously reported [27,28].

The absorption vessel was constructed of glass with an inside diameter of 0.073 m and a height of 0.151 m. Four, equally spaced vertical baffles, each one-tenth of the vessel diameter in width, were attached to the internal wall of the vessel. The gas and liquid phase were agitated with an agitator driven by a 1/4 Hp variable speed motor. A straight impeller 0.034 m in length and 0.05 m in width was used as the liquid phase agitator and located at the middle position of the liquid phase. The surface area of the liquid was calculated as a ratio of the volume (300 cm^3) of added water to the measured height (7.3 cm) of water in the absorber, and its value was 41.096 cm^2. The gas and liquid in the vessel were agitated at 50 rpm, which is enough to keep up a planar gas-liquid interface. The value of the cumulative volume of the soup bubble was measured by a soup bubbler for the change of absorption time to obtain the absorption rate of CO_2. Each experiment was duplicated at least once under identical conditions. It was assumed that the volumetric rising rate of the soup bubble in the soup bubbler attached to the absorption vessel was equal to the value of absorption rate of CO_2. The absorption experiments were carried out in a range of 0-2.0 kmol/m^3 of PGE and 333-363 K at atmospheric pressure using pure CO_2, 2 g of catalyst, and solvents such as DMA, NMP and DMSO.

A sketch of the experimental setup is presented in Fig. 1. A typical experimental run was carried out as follows:

The vent valve A is initially closed and the purge value B is open. CO_2 is flowed continuously through the absorber D, so as to make sure that the latter is filled with gas at the start of the experiment. During this initial period, the water bath temperature is brought up to the desired value, and the liquid batch is kept in bottle F inside the water bath. At the start of the experiment, the liquid batch is poured into funnel G and the agitator E in D is started. The liquid feed valve C is closed, the purge value B is closed, and the vent valve A is opened, as simultaneously as possible. Measurements are started at the soap film meter H taking care that there are always two soap films in the meter so that a continuous reading of the cumulative volume of gas which has flowed through the soap film meter (V) can be recorded as a function of time. The initial volumetric absorption rate of CO_2 was obtained as a slope of the plots of V vs. time at an initial time.

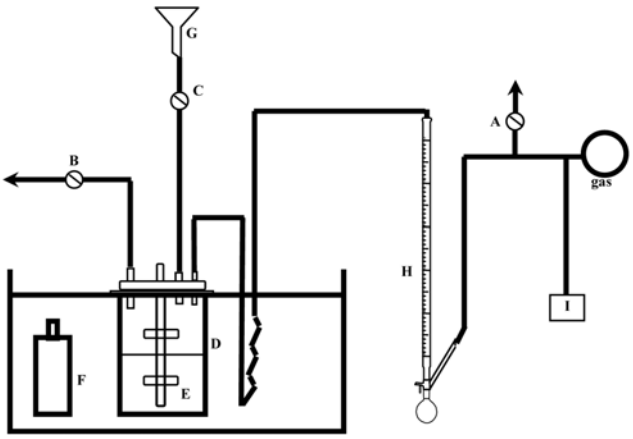

Fig. 1. Schematic of the stirred-cell absorber.

A, B, C. Valve	G. Funnel
D. Absorber	H. Soap film meter
E. Impeller	I. Gas chromatography
F. Liquid bottle	

3. Synthesis of THA-CP-MS41

CP-MS41 was synthesized by hydrolysis of tetraorthosilicate, as a silicon source, with 3-chloropropyltriethoxysilane as an organosilane using cetyltrimethylammonium bromide as a template. THA-CP-MS41 was synthesized by immobilization of trihexylamine on the mesoporous MCM-41. Both synthetic procedures of MCM41 and THA-CP-MS41 followed previous work [20]. The surface area and size of MCM41 were measured by BET isotherm and SEM, and their values were 884.6 m^2/g and 5.0 μm, respectively.

4. Physical Properties

The solubility of CO_2, diffusivity of CO_2 and PGE, and mass transfer coefficient of CO_2 in the PGE solution are needed to solve the simultaneous differential equations, such as Eq. (3) and (4), or Eq. (17) and (18), which were obtained as follows:

The viscosities (μ) of the solvent and the PGE solution were measured using a Brookfield viscometer (Brookfield Eng. Lab. Inc, USA).

The solubility (C_{Ai}) of CO_2 was measured by the pressure measuring method, which involved measuring the pressure difference of CO_2 before and after equilibrium in the gas and liquid phases, similar to a previously reported procedure [29], and the experimental procedure duplicated in detail as previously reported [27].

The diffusivity (D_{io}) of species i in the solvent was estimated by the method modified with viscosity in the Stoke-Einstein equation [30] as follows:

$$D_{io} = 7.4 \times 10^{-12} \frac{TM_S^{1/2}}{\mu^{2/3} V_i} \quad (19)$$

The experimental data [31] were better correlated through the use of two-thirds power of the viscosity in Eq. (19) rather than a power of 1, as shown in Stoke-Einstein equation.

The diffusivity (D_i) of species i in PGE solution, estimated by Eq. (19) using μ of PGE solution.

From measurements of the volume change of CO_2 according to the change of time in the soup bubbler (Fig. 1), the instantaneous mass balance [32] for the mass flux of CO_2 in solvent at a constant

Table 1. Physical properties of the CO_2/PGE system

T (K)	Solvent	C_{Ai} (kmol/m^3)	μ (cp)	$D_{Ao}\times10^9$ (m^2/s)	$D_{Bo}\times10^9$ (m^2/s)	$k_{Lo}\times10^5$ (m/s)
333	DMA	0.0562	0.594	3.921	1.403	3.994
	NMP	0.0593	0.854	3.283	1.175	2.697
	DMSO	0.0528	1.082	2.489	0.890	2.633
343	DMA	0.0494	0.521	4.407	1.577	4.597
	NMP	0.0587	0.691	3.895	1.393	3.026
	DMSO	0.0524	0.761	3.242	1.160	3.136
353	DMA	0.0387	0.468	4.872	1.743	5.122
	NMP	0.0582	0.603	4.389	1.570	3.269
	DMSO	0.0520	0.498	4.426	1.583	3.860
363	DMA	0.0315	0.445	5.181	1.854	5.344
	NMP	0.0578	0.508	5.060	1.810	3.601
	DMSO	0.0517	0.345	5.813	2.080	4.625

Table 2. Experimental data in the CO_2/PGE system

Solvent	C_{Bo} (kmol/m^3)	T (K)	μ (cP)	dv/dt (cm^3/s)	T (K)	μ (cP)	dv/dt (cm^3/s)
DMA	0	333	0.594	0.2294	353	0.468	0.2358
	0.1		0.598	0.2336		0.470	0.2463
	0.5		0.615	0.2433		0.476	0.2625
	1.0		0.628	0.2500		0.484	0.2674
	2.0		0.656	0.2558		0.496	0.2732
	0	343	0.521	0.2625	363	0.445	0.2358
	0.1		0.523	0.2688		0.447	0.2488
	0.5		0.527	0.2809		0.453	0.2653
	1.0		0.531	0.2874		0.460	0.2703
	2.0		0.543	0.2924		0.473	0.2740
NMP	0	333	0.854	0.1795	353	0.603	0.2262
	0.1		0.861	0.1862		0.609	0.2525
	0.5		0.894	0.2033		0.637	0.2994
	1.0		0.923	0.2151		0.663	0.3205
	2.0		0.992	0.2268		0.722	0.3378
	0	343	0.691	0.2053	363	0.508	0.2545
	0.1		0.696	0.2188		0.539	0.3040
	0.5		0.719	0.2475		0.602	0.3745
	1.0		0.743	0.2632		0.663	0.4016
	2.0		0.795	0.2770		0.722	0.4202
DMSO	0	343	1.082	0.1560	353	0.498	0.2387
	0.1		1.084	0.1621		0.499	0.2646
	0.5		1.098	0.1789		0.500	0.3185
	1.0		1.108	0.1912		0.502	0.3448
	2.0		1.134	0.2041		0.505	0.3676
	0	353	0.761	0.1901	363	0.345	0.2924
	0.1		0.763	0.2028		0.348	0.3436
	0.5		0.770	0.2336		0.354	0.4274
	1.0		0.777	0.2532		0.361	0.4608
	2.0		0.793	0.2710		0.370	0.4878

pressure and temperature gives:

$$N_{Ao} = \frac{P}{RTA}\frac{dV}{dt} = k_{Lo}(C_{Ai} - C_A) \quad (20)$$

From Eq. (20) and Henry's law, k_{Lo} at the initial time is obtained:

$$k_{Lo} = \frac{P}{C_{Ai}RTA}\left(\frac{dV}{dt}\right)_{t=0} \quad (21)$$

The values of the mass transfer coefficients (k_{Lo}) of CO_2 in various solvents were obtained from Eq. (21).

The mass transfer coefficient (k_{Loc}) in reactant PGE solution cannot be measured given the reaction of CO_2 with PGE. In this study, k_{Loc} was estimated using the relationship between the mass transfer coefficient (k_{Lo}) with a solvent and diffusivity ratio of D_A to D_{AS} as following [32]:

$$k_{Loc} = k_{Lo}(D_A/D_{AS})^{2/3} \quad (22)$$

The values of μ, C_{Ai}, D_{Ao}, D_{Bo}, and k_{Lo} are listed in Table 1.

RESULTS AND DISCUSSION

The initial volumetric absorption rates (dv/dt) of CO_2 were obtained in a range of 0-2.0 kmol/m^3 of PGE and 333-363 K at atmospheric pressure using pure CO_2, 2 g of catalyst, solvents such as DMA, NMP and DMSO, and are listed in Table 2.

The experimental enhancement factor (β_{exp}), due to the chemical reaction in gas absorption, was obtained as the ratio of dv/dt with reaction to that without reaction.

Fig. 2 shows typical plots of β_{exp} against C_{Bo} in NMP for the experimental parameter of temperature with symbols.

As shown in Fig. 2, β_{exp} increases with increasing C_{Bo} and temperature. These results are exhibited equally for other solvents. The calculated value (β_{cal}) of the consecutive reaction model and the overall reaction model are shown as symbols of the solid and dotted line in Fig. 2, respectively, to be discussed later. As shown in Fig. 2, β_{exp} approaches to both β_{cal} very well within r^2 of 0.9947.

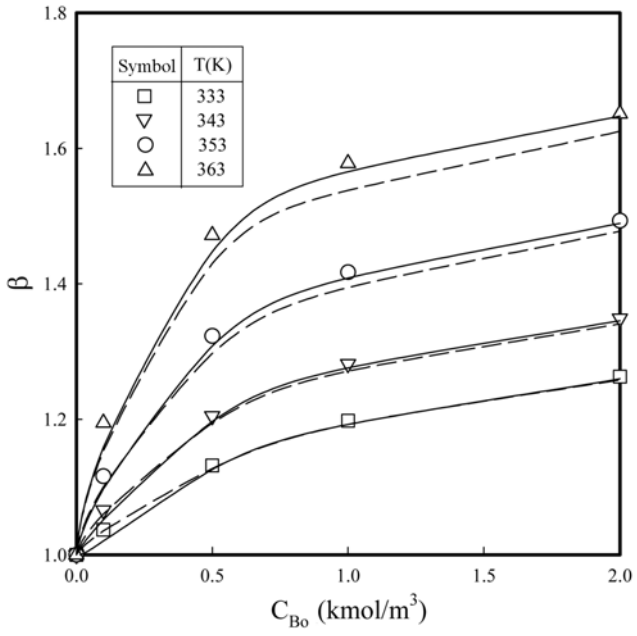

Fig. 2. Enhancement factor vs. C_{Bo} in NMP at various temperatures.

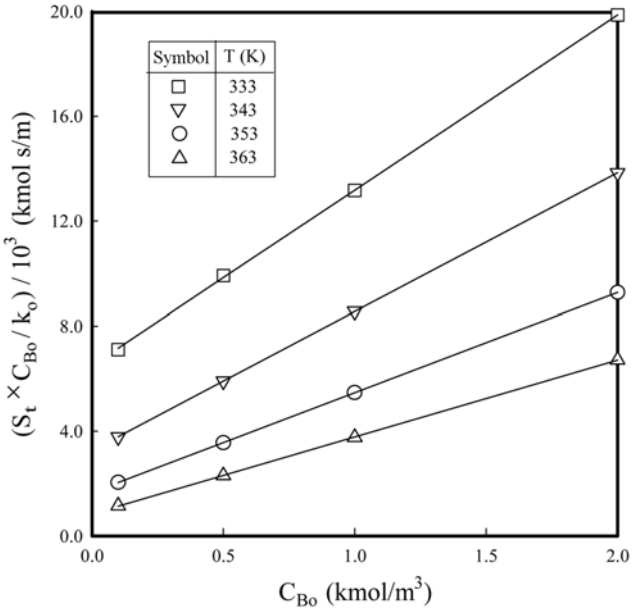

Fig. 3. S_tC_{Bo}/k_o vs. C_{Bo} with the same conditions shown in Fig. 2.

To evaluate k_3 and K_1, k_o is obtained from β_{exp} and Eq. (13). Typical plots of S_tC_{Bo}/k_o against C_{Bo} are presented in Fig. 3 for the same conditions as shown in Fig. 2.

As shown in Fig. 3, the plots satisfy a straight line and k_3 and K_1 are obtained from the slope and intercept of the straight line according to Eq. (10), respectively. These results are exhibited equally for other solvents. The values of k_3, K_1 and k_{max} for various solvents and temperatures are listed in Table 3.

Fig. 4 shows the Arrhenius plots of k_3 for various solvents using data in Table 3.

As shown in Fig. 4, the Arrhenius plots are linear, and the linear regression analysis of the Arrhenius plots with r^2>0.9960 gives the activation energy for the forward reaction rate constant in the irreversible reaction of (iii), with 30.9, 28.1, 27.3 kJ/mol for DMA, NMP,

Table 3. Reaction rate constants of the reaction between CO_2 and PGE

T (K)	Solvent	$k_3\times10^4$ (1/m^2·s)	K_1 (1/M)	$k_{max}\times10^4$ (1/M·m^2·s)
333	DMA	0.912	1.294	1.180
	NMP	1.495	1.030	1.540
	DMSO	2.483	0.803	1.994
343	DMA	1.175	1.979	2.325
	NMP	1.890	1.621	3.064
	DMSO	3.400	1.141	3.879
353	DMA	1.702	3.059	5.206
	NMP	2.626	2.291	6.016
	DMSO	4.446	1.663	7.394
363	DMA	2.247	4.392	9.869
	NMP	3.411	3.440	11.761
	DMSO	5.613	2.505	14.061

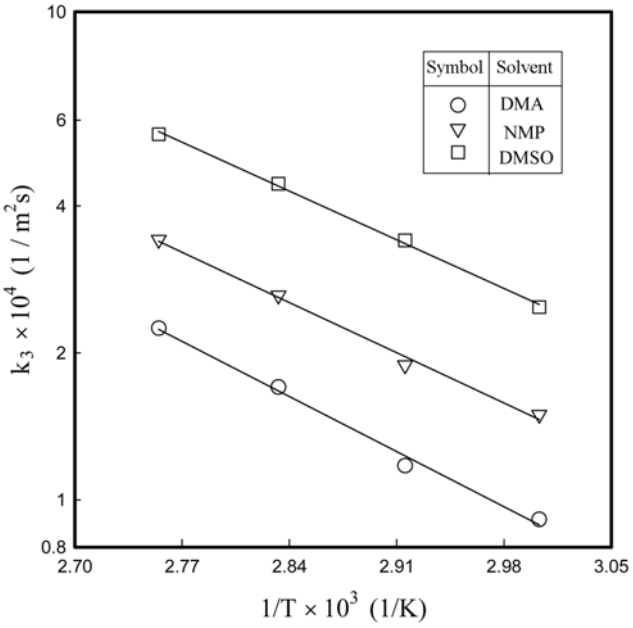

Fig. 4. Arrhenius plot of the CO_2-PGE system.

and DMSO, respectively.

Various empirical measurements of the solvent effects have been proposed and correlated with the reaction rate constant [33]. Of these, some measurements have a linear relation to the solubility parameter (δ) of the solvent with logarithms of k_3 and K_1 plotted against δ [34] of DMA, NMP, and DMSO, 22.1, 23.1, 24.6 $(J/m^3)^{0.5}$, respectively, in Fig. 5.

As shown in Fig. 5, the plots are linear, and k_3 and K_1 increase and decrease with increasing δ, respectively. The solvent polarity increased with increasing δ. It can be assumed that increased instability and solvation of complex (C_1), arising from increased solvent polarity, enhance the dissociation reaction of C_1 and the reaction between C_1 and CO_2, as in an SN_1 (nucleophilic substitution) reaction [35]. From the results in Fig. 5, the magnitude of the rate constants may be a function of the degree to which the solvent was able to stabilize the zwitterionic intermediates [4].

To compare the chemical kinetics of the consecutive reaction with those of the overall reaction, the enhancement factors (β_{cal}) of both the consecutive reaction and the overall reaction can be estimated using Eq. (8) and the solution of the simultaneous differential equations of Eq. (3) and (4) in the consecutive reaction, and Eq. (17) and (18) in the overall reaction, respectively. These differential equations were numerically solved by a finite element method with the boundary conditions of Eq. (5) and (6) using the physicochemical properties in Tables 1 and 3. β_{cal} in NMP at various temperatures are shown as symbols of the solid and dotted lines for both the models in Fig. 2. All values of β_{exp} and β_{cal} for various C_{Bo}, and temperatures in various solvents are plotted in Fig. 6 to compare with each other.

As shown in Fig. 6, β_{exp} approached β_{cal} very well within a mean deviation of 0.80% and standard deviation of 0.011% with r^2 of 0.9977 for the consecutive reaction model and within a mean deviation of 0.92% and standard deviation of 0.018% with r^2 of 0.9947 for the overall reaction model, respectively. From a comparison of the overall reaction rate of Eq. (15) with the consecutive reactions of Eq. (2) using the viewpoint of these statistics as mentioned above, the reaction kinetics between CO_2 and PGE with a catalyst, consisting of 2-step consecutive reactions can be treated as those of an overall reaction of CO_2 and PGE with the overall reaction constant of a form similar to Michaelis-Menten enzyme kinetics or the Langmuir adsorption isotherm, i.e., the pseudo-first-order reaction constant in the consecutive reaction model can be used to evaluate the overall reaction rate constant.

Fig. 7 shows the Arrhenius plots of k_{max} for various solvents using data in Table 3. As shown in Fig. 7, the Arrhenius plots are linear and the linear regression analysis of the Arrhenius plots with r^2>

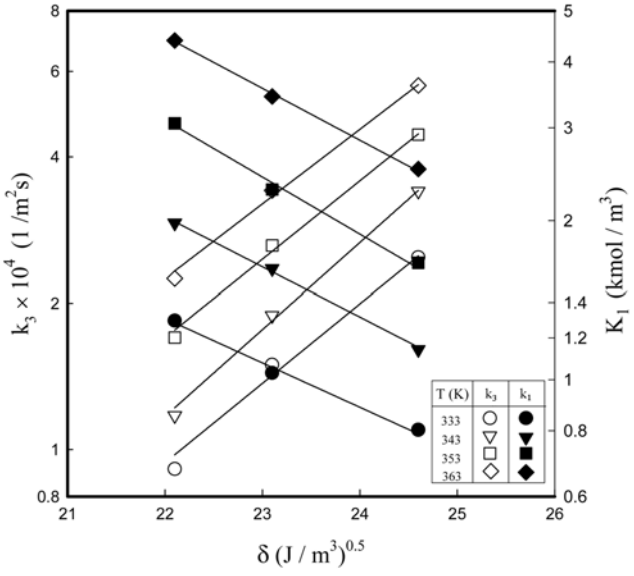

Fig. 5. Relationship between reaction rate constant and solvent solubility parameter.

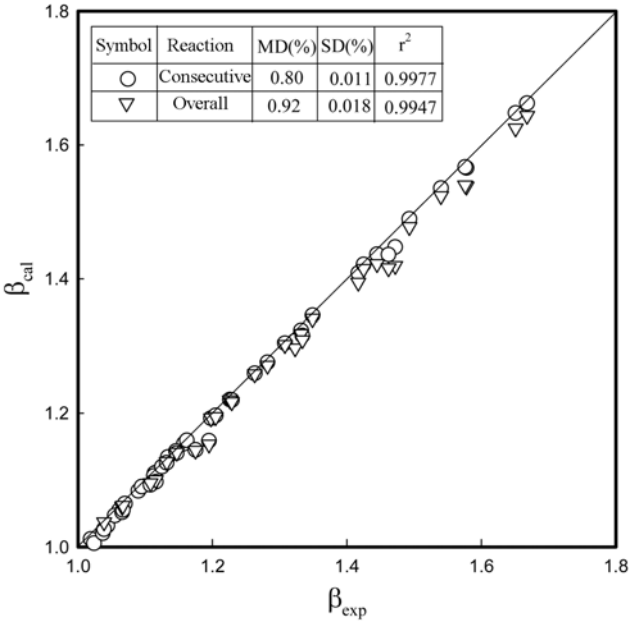

Fig. 6. Comparison of the calculated and measured values of the enhancement factor of CO_2.

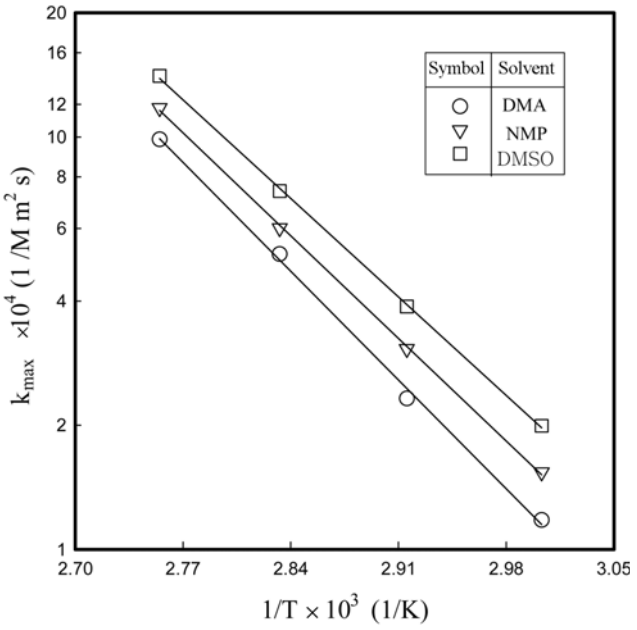

Fig. 7. Arrhenius plot of k_{max} in the CO_2-PGE system for various solvents.

0.9992 gives the empirical formulas for DMA, NMP, and DMSO, respectively.

$k_{max}=2.38\times10^7 \exp(-8.67\times10^3/T)$ for DMA
$k_{max}=7.23\times10^6 \exp(-8.19\times10^3/T)$ for NMP
$k_{max}=3.50\times10^6 \exp(-7.86\times10^3/T)$ for DMSO

CONCLUSIONS

Carbon dioxide was absorbed to react with a PGE solution of DMA, NMP, and DMSO in a flat-stirred vessel at 101.3 kPa. Two mathematical models for CO_2 absorption into the PGE solution were developed on the basis of the film theory accompanied by 2-step consecutive reactions according to the zwitterion mechanism and the overall reaction, respectively. Absorption data of CO_2 were used to obtain pseudo-first-order reaction rate constants, from which the elementary reaction rate constants and the overall reaction rate constant were evaluated. It was found that the dependence of the logarithms of the consecutive reaction rate constants on the solubility parameter of the solvent was close to linear.

ACKNOWLEDGEMENTS

This work was supported by the Korea Ministry of Environment (MOE) as a Human resource development Project for Waste to Energy, a grant (2006CCD11P011A-21-3-010) from Energy Technology R&D of the Korea Energy Management Corporation, and the National Research Foundation of Korea Grant founded by the Korean Government (NRF-2009-K20601000004-00410).

NOMENCLATURE

a_v : ratio of interfacial area of liquid to liquid volume [1/m]
C_i : concentration of species i [M]
D_i : diffusivity of species i [m^2/s]
k_{max} : specific overall reaction rate constant with maximum of k_{over} (1/M·m^2·s)
k_o : pseudo-first-order reaction rate constant [1/s]
k_{over} : overall reaction rate constant [1/Ms]
K_1 : reaction equilibrium constant defined as k_1/k_2 [1/M]
k_1 : forward reaction rate constant in reaction (ii) [1/m^2·s]
k_2 : backward reaction rate constant in reaction (ii) [M/m^2·s]
k_3 : forward reaction rate constant in reaction (iii) [1/m^2·s]
k_{Lo} : liquid-side mass transfer coefficient of CO_2 in solvent [m/s]
k_{Loc} : liquid-side mass transfer coefficient of CO_2 in PGE solution [m/s]
M_s : molecular weight of solvent [kg/kmol]
r^2 : correlation coefficient
$r_{A,\,cons}$: reaction rate of CO_2 in consecutive reaction model [M/s]
$r_{A,\,over}$: reaction rate of CO_2 in overall reaction model [M/s]
S_t : surface area of catalyst [m^2]
t : absorption time [s]
T : absorption temperature [K]
V : cumulative volume of the soup bubble [cm^3]
z : distance [m]
z_L : film thickness [m]

Greek Letters

β : enhancement factor of CO_2
d : solubility parameter of solvent (J/m^3)$^{1/2}$
μ : viscosity of liquid [cP]

Subscripts

A : CO_2
B : PGE
cal : calculated value
exp : measured value
i : gas-liquid interface or species i
L : bulk solution
o : feed or solvent

REFERENCES

1. M. Aresta, *Carbon Dioxide Recovery and Utilization*, Kluwer Academic Publishers, London (2003).
2. K. Weissermel and H. Arpe, *Industrial Organic Chemistry*, Wiley-VCH, Weinheim, New York (1997).
3. W. J. Peppel, *Ind. Eng. Chem*., **50**, 767 (1958).
4. G. Rokicki, *Makromol. Chem*., **186**, 331 (1985).
5. T. Aida and S. Inoue, *J. Am. Chem. Soc*., **105**, 1304 (1983).
6. Y. Nishikubo, T. Kato, S. Sugimoto, M. Tomoi and S. Ishigaki, *Macromolecules*, **23**, 3406 (1990).
7. N. Kihara and T. Endo, *Macromolecules*, **25**, 4824 (1992).
8. T. Nishikubo, A. Kameyama, J. Yamashida, M. Tomoi and W. Fukuda, *J. Polym. Sci., Part A, Polym. Chem*., **31**, 939 (1993).
9. T. Nishikubo, A. Kameyama, J. Yamashida, T. Hukumitsu, C. Maejima and M. Tomoi, *J. Polym. Sci., Part A: Polym. Chem*., **33**, 1011 (1995).
10. C. M. Starks, C. L. Liotta and M. Halpern, *Phase Transfer Cataly-*

sis, Chapmann & Hall, New York (1994).
11. L. K. Daraiswany and M. M. Sharma, *Heterogeneous Reaction: Analysis, Example and Reactor Design*, John Wiley & Sons, New York (1980).
12. C. T. Kresge, M. E. Leonowicz, W. J. Roth, J. C. Vartuli and J. S. Beck, *Nature*, **359**, 710 (1992).
13. J. S. Beck, J. C. Vartuli, W. J. Roth, M. E. Leonowicz, C. T. Kresge, K. D. Schmitt, C. T. W. Chu, D. H. Olson, E. W. Sheppard, S. B. McCullen, J. B. Higgins and J. L. Schlenker, *J. Am. Chem. Soc*., **114**, 10834 (1992).
14. D. Zhao, J. Feng, Q. Huo, N. Melosh, G. H. Fredrickson, B. F. Chmelka and G. D. Stucky, *Science*, **279**, 548 (1998).
15. A. Bhaumik and T. Tatsumi, *J. Catal*., **189**, 31 (2000).
16. S. L. Burkett, S. D. Sim and S. J. Mann, *J. Chem. Soc., Chem. Commun*., 1367 (1996).
17. M. H. Lim, C. F. Blanford and A. Stein, *J. Am. Chem. Soc*., **119**, 4090 (1997).
18. C. E. Fowler, B. Lebeau and S. Mann, *J. Chem. Soc., Chem. Commun*., 1825 (1998).
19. F. Babonneau, L. Leite and S. Fontlupt. *J. Mater. Chem*., **9**, 175 (1999).
20. S. Udayakumar, S. W. Park, D. W. Park and B. S. Choi, *Catal. Commun*., **9**, 1563 (2007).
21. S. W. Park, D. W. Park, T. Y. Kim, M. Y. Park and K. J. Oh, *Catal. Today*, **98**, 493 (2004).
22. S. W. Park and J. W. Lee, *Stud. Surf. Sci. Catal*., **159**, 345 (2006).
23. S. W. Park, B. S. Choi, D. W. Park and J. W. Lee, *J. Ind. Eng. Chem*., **11**, 527 (2005).
24. S. W. Park, B. S. Choi, B. D. Lee, D. W. Park and S. S. Kim, *Sep. Sci., Technol*., **41**, 829 (2006).
25. S. W. Park, B. S. Choi, D. W. Park, K. J. Oh and J. W. Lee, *Green Chem*., **9**, 605 (2007).
26. S. W. Park, B. S. Choi, D. W. Park, S. Udayakumar and S. J. Lee, *Catal. Today*, **131**, 559 (2008).
27. Y. S. Son, S. W. Park, D. W. Park, K. J. Oh and S. S. Kim, *Korean J. Chem. Eng*., **26**, 783 (2009).
28. W. Yu, G. Astarita and D. W. Savage, *Chem. Eng. Sci*., **40**, 1585 (1985).
29. M. L. Kennard and A. Meisen, *J. Chem. Eng. Data*, **29**, 309 (1984).
30. R. C. Reid, J. M. Prausnitz and T. K. Sherwood, *The properties of Gases and Liquid*, McGraw-Hill Book Company, New York (1977).
30. E. L. Cussler, *Diffusion*, Cambridge University Press, New York (1984).
32. G. Carta and R. L. Pigford, *Ind. Eng. Chem. Fundam*., **22**, 329 (1983).
33. H. F. Herbrandson and F. B. Neufeld, *J. Org. Chem*., **31**, 1140 (1966).
34. J. Brandrup and E. H. Immergut, *Polymer Handbook*, Second Ed., John Wiley & Sons, New York (1975).
35. R. T. Morrison and R. N. Boyd, *Org. Chem.*, Fourth Ed., Allyn and Bacon, Inc, Toronto (1983).